Published online April 12, 2018

A Comprehensive Model for Single Ring Infiltration I: Initial Water Content and Soil Hydraulic Properties

Ryan D. Stewart*
Dep. of Crop and Soil
Virginia Polytechnic Inst. and State Univ.
Environmental Science
Blacksburg, VA 24061

Majdi R. Abou Najm
Dep. of Civil and Environ. Engineering
American Univ. of Beirut
Beirut, Lebanon

Single ring infiltration tests are commonly used to understand soil hydraulic properties. While a number of models have been developed to describe three-dimensional infiltration from single ring sources, these expressions are often restricted to cases where the soil is initially dry and the source pressure head is negligible. These conditions may restrict the use of these expressions in real field settings. In this study we modified a set of infiltration models to explicitly account for variations in soil hydraulic properties, initial conditions, and experimental setups. The resultant expressions allowed us to explore how soil capillary length (a measure of the capillary force acting through the wetted zone) and three-dimensional wetting profiles vary under different initial matric heads. Specifically, as initial matric head increases, infiltration becomes increasingly one-dimensional due to a decrease of the soil capillary force. However, for most realistic situations (i.e., moderately wet to very dry initial conditions) the model can be simplified by assuming a constant capillary length. The resulting expressions compared well with numerical results from HYDRUS-3D for five different soils, including both dry and wet initial conditions, two ring insertion depths, and two ponding depths. Overall, the model provides further insight on the variations in soil capillarity (as sorptivity) and infiltration across a range of soil types and initial conditions, and can be used to describe single ring infiltration under nearly every scenario.

Core Ideas

- **New single ring infiltration model accounts for a wide range of experimental conditions.**
- **Soil capillarity as function of initial water content was explored.**
- **Model closely matched HYDRUS-3D simulations for thirty infiltration scenarios.**
- **Model was tested with both Brooks and Corey and van Genuchten–Mualem hydraulic parameters.**
- **Brooks and Corey parameters gave more consistent predictions for cumulative infiltration.**

Infiltration tests are often used to determine soil physical properties such as field-saturated hydraulic conductivity, K_{fs}, which has led to the development of numerous approaches to measure infiltration rates in the field. Examples of infiltration methods include single ring (Castellini et al., 2016; Reynolds and Elrick, 1990) and double ring (Fatehnia et al., 2016; Pollalis and Valiantzas, 2014) infiltrometers that use a circular ponded water source at the soil surface; tension infiltrometers (Reynolds and Elrick, 1991; Shuster et al., 2015) that use a cylindrical water source under negative pressure at the soil surface; borehole permeameters that allow water to infiltrate from within an auger hole (Elrick and Reynolds, 1992; Hinnell et al., 2009); and the air-entry permeameter (Bouwer, 1966), in which the soil capillary force is quantified during the infiltration process. Each approach requires a distinct set of assumptions and supplementary information to decipher hydraulic properties from the infiltration results.

Single ring infiltration tests offer the advantages of being easy to conduct and requiring minimal and inexpensive equipment. However, interpreting or predicting infiltration from single ring infiltrometers requires solutions that account for the three-dimensional flow patterns in the soil. In particular, knowledge of the soil capillary force is needed to interpret early-time and steady infiltration behavior and predict infiltration (Stewart et al., 2013).

Two main groups of solutions have emerged that explicitly predict infiltration and infiltration rates as functions of time (Table 1). The first, developed by Haverkamp et al. (1990), Haverkamp et al. (1994), uses the soil water diffusivity to predict three-dimensional wetting behaviors as encapsulated by a shape parameter γ.

Soil Sci. Soc. Am. J.
doi:10.2136/sssaj2017.09.0313
Received 8 Sept. 2017.
Accepted 7 Feb. 2018.
*Corresponding author (ryan.stewart@vt.edu).
© Soil Science Society of America, 5585 Guilford Rd., Madison WI 53711 USA. All Rights reserved.

The Haverkamp solution is valid for all time, and has subsequently been modified to interpret soil hydraulic properties from slightly ponded ring infiltration tests, in a process known as the Beerkan Estimation of Soil Transfer Properties (BEST). BEST analyses have successively been used to analyze infiltration tests and predict hydraulic properties such as K_{fs}. However, the solutions do not allow flexibility in the choice of soil hydraulic model (i.e., water retention is specified using van Genuchten parameters while unsaturated hydraulic conductivity is prescribed with the Brooks and Corey parameter set). The BEST methods, as developed by Braud et al. (2005); Lassabatère et al. (2006), also require measurement of a particle size distribution to be fully utilized. Finally, the Haverkamp model was developed for tension infiltration sources, where the source pressure head is less than zero and the disc source rests on the soil surface, making it less accurate in situations where source pressure or depth of ring insertion are positive.

The other family of three-dimensional infiltration models are similar in form to the Wooding (1968) solution, and are valid for steady-state infiltration conditions. For example, Reynolds and Elrick (1990) developed a steady-state model that accounts for differences in ring geometries, insertion depths, and water supply ponding depths. This infiltration model was later modified using two additional empirical parameters to predict early- and transient-time infiltration behaviors (Wu et al., 1999), which removed the requirement of steady-state conditions. The ability to account for different ponding depths allows the model to reflect various experimental configurations, where relatively high supply heads may be used to optimize analysis stability, reduce measurement times (Reynolds et al., 2002), and better mimic natural rainfall (Di Prima et al., 2017).

In this study we build on the Wu et al. (1999) and Reynolds and Elrick (1990) solutions to propose a comprehensive infiltration model for single ring sources, with the ultimate goal of being able to describe infiltration into a range of soil types and initial conditions with minimal auxiliary data. The proposed model accounts for different ring sizes and depths of insertion, initial water content and matric pressure head, transient and steady-state infiltration behaviors, and non-zero water supply pressures. As such, it has considerable flexibility when compared with other models.

Theory

Infiltration Model

Based on two-term Philip type solutions matched for short and long times (Philip, 1987), infiltration I [L] from a single ring source can be described as:

$$I = c_1\sqrt{t} + c_2 t \qquad t < \tau_{crit} \qquad [1a]$$

$$I = c_3 + c_4 t \qquad t \geq \tau_{crit} \qquad [1b]$$

$$\tau_{crit} = \frac{1}{4}\left(\frac{c_1}{c_4 - c_2}\right)^2 \qquad [1c]$$

where c_1 [L T$^{-0.5}$], c_2 [L T^{-1}], c_3 [L] and c_4 [L T^{-1}] are constants, and τ_{crit} [T] represents the time of transition between early-time and steady-state infiltration behaviors. Note that in Eq. [1c] τ_{crit} is defined as the time when the infiltration rate (dI/dt) is equal between Eq. [1a] and [1b].

In many formulations, such as those of Haverkamp et al. (1994) and Philip (1969), the c_1 term is taken to be equal to the soil sorptivity, S [L T$^{-0.5}$]. Using the White and Sully (1987) expression for sorptivity, we obtain:

$$c_1 = S = \sqrt{(\theta_s - \theta_i)(h_{source} + \lambda)K_{fs}/b} \qquad [2]$$

where θ_i and θ_s represent the respective initial (i.e., background) and saturated soil water contents, h_{source} is the pressure head at the source [L], K_{fs} is the field-saturated hydraulic conductivity [L T^{-1}], and b is a parameter (White and Sully, 1987) that varies between 1/2 and $\pi/4$ depending on the shape of the soil water diffusivity function. A value of b = 0.55 is often assumed (Haverkamp et al., 1994; Reynolds and Elrick, 1990; White and Sully, 1987). λ is the capillary length [L] (a measure of the soil capillary force), which we define as being equal to the matric flux potential, Λ, scaled by K_{fs}:

$$\lambda = \Lambda / K_{fs} \qquad [3]$$

Note that the capillary length term defined in Eq. [3] can be considered to be the reciprocal of the α^* parameter used in other studies (Angulo-Jaramillo et al., 2016; Reynolds et al., 2002).

The matric flux potential [L^2 T^{-1}] is a macroscopic measure of the averaged capillary force acting through the wetted soil, and can be found by (Gardner, 1958; Philip, 1984):

Table 1. Saturated water content (θ_s), residual water content (θ_r), saturated hydraulic conductivity (K_s), bubbling pressure head (h_b), pore size index (η), and empirical fitting parameters (α, m, and n) for the eight soils used in comparisons and analysis. Original source: Fuentes et al. (1992).

No.	Soil	θ_s	θ_r†	K_s	h_b	η	α	m	n
				cm min^{-1}	cm		cm^{-1}		
1	Guelph loam	0.52	0.17, 0.22	0.022	−45.82	3.56	0.0115	0.51	2.04
2	Yolo light clay	0.50	0.0, 0.0	0.00074	−16.56	2.62	0.0325	0.21	1.26
3	Grenoble sand	0.31	0.0, 0.0	0.26	−11.43	5.86	0.0432	0.51	2.04
4	Columbia silt‡	0.40	0.0, 0.0	0.0035	−6.657	5.45	0.0176	0.26	1.34
5	Hygiene sandstone	0.25	0.13, 0.15	0.075	−105.35	10.84	0.00793	0.90	10.4
6	Touchet silt loam	0.47	0.12, 0.19	0.21	−148.80	7.23	0.00505	0.87	7.63
7	Silt loam G.E.3	0.40	0.013, 0.13	0.0035	−128.48	3.16	0.00423	0.51	2.06
8	Beit Netofa clay	0.45	0.089, 0.29	5.7×10^{-5}	−208.04	2.39	0.00202	0.37	1.59

† The first value is Brooks and Corey model, the second value is van Genuchten–Mualem model.

‡ h_b and η were set so that the maximum capillary length (λ_{max}) and maximum matric flux potential (Λ_{max}) were equivalent between the Brooks and Corey and van Genuchten–Mualem parameters.

$$\Lambda = \int_{h_i}^{0} K(h)\,dh \qquad [4]$$

where $K(h)$ is hydraulic conductivity [L T^{-1}] as a function of matric head, h [L], integrated between the initial condition h_i (where $h_i < 0$) and saturated conditions ($h = 0$).

In the case of three-dimensional ponded infiltration from a single ring source, Wu et al. (1999) determined an empirical infiltration equation with the general form of Eq. [1]. In their solution, the c_2 term is equal to:

$$c_2 = afK_{fs} \qquad [5]$$

where a is a constant and f is a factor related to the three-dimensional wetting shape. Using the analysis of Reynolds and Elrick (1990), f can be described as:

$$f = \frac{h_{source} + \lambda}{d + r_d/2} + 1 \qquad [6]$$

where d is the depth of ring insertion [L] and r_d is the single ring disk radius [L].

The original Reynolds and Elrick (1990) analysis, done for steady-state conditions, suggested the c_4 term can be defined as:

$$c_4 = fK_{fs} \qquad [7]$$

Because cumulative infiltration must be continuous at time τ_{crit} (i.e., Eq. [1a] and [1b] must equal each other at the time of transition), we can substitute Eq. [2], [5] and [6] into Eq. [1] and solve for c_3. Equation [1] then becomes:

$$I = \sqrt{(\theta_s - \theta_i)(h_{source} + \lambda)K_{fs}/b}\sqrt{t} + afK_{fs}t \quad t < \tau_{crit} \qquad [8a]$$

$$I = \frac{(\theta_s - \theta_i)(h_{source} + \lambda)}{4fb(1-a)} + fK_{fs}t \quad t \geq \tau_{crit} \qquad [8b]$$

$$\tau_{crit} = \frac{(\theta_s - \theta_i)(h_{source} + \lambda)}{4bK_{fs}f^2(1-a)^2} \qquad [8c]$$

In the original development of the Wu and Pan (1997) model, a was determined through curve-fitting to be approximately equal to 0.91. Here, we instead use the definitions of Eq. [2] and [6] to rewrite Eq. [8a] as:

$$I = S\sqrt{t} + aK_{fs}t + \frac{S^2ab}{(\theta_s - \theta_i)(d + r_d/2)}t \quad t < \tau_{crit} \qquad [8d]$$

In Eq. [8d], as the depth of ring insertion, d, and/or the disk radius, r_d, go to infinity, the last term of the right hand side becomes 0, while at the same time water flow from the disk source becomes one-dimensional. In that case, $I = S\sqrt{t} + aK_{fs}t$, which corresponds to the first two terms of the Philip (1957) model for one-dimensional vertical infiltration. Real soils have been shown to have values of $0.4 < a < 0.5$ (Philip, 1990), so based on this result and our subsequent analysis we recommend using a mean value of $a = 0.45$. Thus, our recommended a value is approximately one half of the value recommended by Wu and Pan (1997).

Capillary Length

While the capillary length, λ, can be determined experimentally, such as by using two rings with different radii (Scotter et al., 1982) or by assuming a value dependent on soil texture and structure (Reynolds et al., 2002), here we focus on quantifying λ via an analytical approach. To solve Eq. [4], we need a model for $K(h)$; we choose the Brooks and Corey (1964) model, noting that other hydraulic models can instead be used but may require numerical integration to solve. The Brooks and Corey (1964) solutions for water content θ and $K(h)$ as functions of pressure head h are:

$$\theta = (\theta_s - \theta_r)(h_b/h)^{(\eta-2)/3} + \theta_r \quad h < h_b \qquad [9a]$$

$$\theta = \theta_s \quad h \geq h_b \qquad [9b]$$

and

$$K(h) = K_{fs}(h_b/h)^{\eta} \quad h < h_b \qquad [10a]$$

$$K(h) = K_{fs} \quad h \geq h_b \qquad [10b]$$

where h_b is the bubbling pressure head [L] (with the constraint $h_b < 0$), η is a pore size index (with the constraint $\eta > 2$), and θ_r is the residual water content.

Evaluating Eq. [3] using Eq. [4] and [10] gives:

$$\lambda = \int_{h_b}^{0} dh + \int_{h_i}^{h_b} (h_b/h)^{\eta}\,dh = \left(\frac{h_b\eta - h_i(h_b/h_i)^{\eta}}{1-\eta}\right) \quad h_i < h_b \qquad [11a]$$

$$\lambda = \int_{h_i}^{0} dh = -h_i \quad h_i \geq h_b \qquad [11b]$$

As the soil becomes very dry, λ will converge to a maximum value λ_{max}:

$$\lambda_{max} = h_b\eta/(1-\eta) \qquad [12]$$

The validity of the assumption that $\lambda \approx \lambda_{max}$ can be evaluated by examining how the ratio of λ/λ_{max} varies as a function of initial matric head. Combining Eq. [11] and [12], we define this ratio as:

$$\frac{\lambda}{\lambda_{max}} = \left(\frac{h_b\eta - h_i(h_b/h_i)^{\eta}}{h_b\eta}\right) = 1 - \frac{1}{\eta}\left(\frac{h_i}{h_b}\right)^{1-\eta} \quad h_i < h_b \qquad [13a]$$

$$\frac{\lambda}{\lambda_{max}} = \frac{-h_i}{h_b\eta/(1-\eta)} = \frac{\eta-1}{\eta}\left(\frac{h_i}{h_b}\right) \quad h_i \geq h_b \qquad [13b]$$

Note that the ratio λ/λ_{max} also provides a relative indication of the extent of three-dimensional flow: as h_i goes to zero (i.e., as the initial soil water content increases toward saturation), λ/λ_{max} also goes to zero, thus indicating one-dimensional vertical flow. This condition is more theoretical than practical, as such conditions would only occur with saturated yet draining conditions (e.g., rain falling on the soil surface at a rate equivalent to K_{fs} and a water supply value $h_{source} \approx 0$). Still, this analysis reveals that the capillary length decreases from a maximum in very dry soils toward small values in nearly-saturated soils.

Three-dimensional Wetting Shape Factor

Here we again use Brooks and Corey parameters to develop an expression for the three-dimensional wetting shape factor, f, noting again that other hydraulic models can be used instead. Substituting Eq. [10] into Eq. [6] results in:

$$f=\frac{h_{source}(1-\eta)+h_b\eta-h_i(h_b/h_i)^{\eta}}{(d+r_d/2)(1-\eta)}+1 \qquad h_i<h_b \quad [14a]$$

$$f=\frac{h_{source}-h_i}{(d+r_d/2)}+1 \qquad h_i\geq h_b \quad [14b]$$

In very dry conditions, Eq. [14] can be simplified, as f will converge to a maximum value f_{max}:

$$f_{max}=\frac{h_{source}(1-\eta)+h_b\eta}{(d+r_d/2)(1-\eta)}+1 \quad [15]$$

METHODS

Numerical Simulations with Synthetic Soils

Relative capillary length (λ/λ_{max}) was quantified for four synthetic soils, with Brooks and Corey parameter η = 2.5, 4, 8, and 16, by evaluating Eq. [13] over the range of scaled initial matric head $0 \leq h_i/h_b \leq 1000$. We also explored how λ_{max} varies as a function of the Brooks and Corey parameters h_b and η, by calculating Eq. [12] for a wide range of parameter values. To provide additional context, we included eight well-characterized soils as summarized by Fuentes et al. (1992) (Table 1).

We also evaluated the infiltration model and its associated parameters using the van Genuchten (1980) water retention and hydraulic conductivity models:

$$\theta=(\theta_s-\theta_r)\left(1+|\alpha h|^n\right)^{-m}+\theta_r \quad [16]$$

$$K(h)=K_{fs}\left(1-|\alpha h|^{n-1}\left[1+|\alpha h|^n\right]^{-m}\right)^2\left(\left[1+|\alpha h|^n\right]^{-m/2}\right) \quad [17]$$

where α, m, and n are empirical parameters. To our knowledge, there is not a simple closed-form analytical solution for capillary length using the van Genuchten–Mualem function (e.g., the equivalent of Eq. [11]). To determine the applicable values for λ based on van Genuchten–Mualem parameters, we numerically integrated Eq. [4] using Eq. [17] as the $K(h)$ function. We accomplished this using the default integrate option in the software package R (version 3.3.1); note that we evaluated the precision of the numerical integration tool by specifying absolute tolerances of 0.001, 0.00001, and 0.0000001 for the same parameter set, which showed no differences in the result (to at least 6 significant figures).

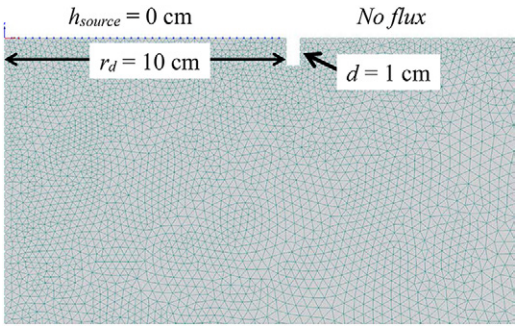

Fig. 1. Screenshot of HYDRUS-2D/3D model of a single ring infiltration source (blue dots on upper left surface), with simulated ring insertion depth of 1 cm.

For the subsequent analysis, n was set to 1.1, 1.5, 2, and 4, and m was constrained using the Mualem constraint $m = 1 - 1/n$ (van Genuchten, 1980). h_i was scaled by multiplying it by α over the range $0 \leq \alpha h_i \leq 1000$. The diffusivity shape parameter b was again set equal to 0.55.

Numerical Simulations with HYDRUS-3D

The proposed infiltration model (Eq. [8]) was evaluated using numerical simulations, created within HYDRUS-3D (Version 2.05.0250), of single ring infiltration experiments. The model domain was an axisymmetric (x-z) plane of 100-cm radius by 200-cm depth. 47,739 nodes were used, ranging from a node spacing of 0.25 cm near the origin to 1.5 cm at the far edge of the domain. A single ring infiltration source of 10-cm disk radius (r_d = 10 cm) was modeled at the upper origin with depth of insertion d = 1 cm, using a constant head condition of h_{source} = 0 cm at the top. A no-flux boundary condition was used to simulate the thickness of the inserted ring (Fig. 1). The remaining boundary nodes were set to no flux conditions. The first four of the soils from Table 1 (Guelph loam; Yolo light clay; Grenoble sand; Columbia Silt) and the Silt loam G.E.3 soil were modeled using the Brooks and Corey and van Genuchten hydraulic functions. For the Guelph loam, Yolo light clay, and Grenoble sand soils, we used the parameters quantified by Fuentes et al. (1992). With the Columbia silt, we used the van Genuchten parameters from Fuentes et al. (1992), but then set the Brooks and Corey hydraulic parameters such that the maximum capillary length λ_{max} was equivalent between the two hydraulic models (using least-squares fitting on Eq. [12], whereby the parameters h_b and η were adjusted). We also performed additional simulations where the depth of ring insertion d was set equal to 5 cm and h_{source} was set to be 0 cm and 25 cm, using only the Brooks and Corey parameter sets.

The predicted infiltration for every hydraulic parameter set was evaluated under both initially dry (h_i = −5000 cm) and wet (h_i = −50 cm for the first four soils; h_i = −130 cm for the Silt loam G.E.3 soil) conditions. Each run simulated a 500-min infiltration event. For the case of the Brooks and Corey parameters, we evaluated Eq. [8] using the expressions developed in Eq. [11] and [14], assuming b = 0.55 and a = 0.45. The van Genuchten-Mualem parameters again required numerical integration in the software package R (version 3.3.1) to determine the capillary length λ for each simulation. We then used those estimated λ values to calculate f (Eq. [6]), and substituted that value into Eq. [8].

To quantify the relative error of our infiltration model compared with the HYDRUS results, we used the coefficient of variation of the root mean square deviation, CV(RMSD):

$$CV(RMSD)=\frac{\sqrt{\sum_{i=1}^{N}(\hat{y}_i-y_i)^2/n}}{y_{total}} \quad [18]$$

where $\hat{y}_i$ is the cumulative infiltration predicted by the proposed model at time i, y_i is the cumulative infiltration predicted by HYDRUS at time i, n is the number of predicted values, and y_{total} is the total cumulative infiltration at 500 min. Note that we selected y_{total} to normalize RMSD values since total infiltration depths varied over two orders of magnitude between soil types. The CV(RMSD) values thus approximated overall model error as a fraction of total infiltration. In other words, a CV(RMSD) value of 0.1 indicated the model error was ~10% of the total infiltration amount.

We also compared infiltration predictions from both HYDRUS and Eq. [8] with the early-time solution of Haverkamp et al. (1994):

$$I_{\text{Haverkamp}} = S\sqrt{t} + \left[K_i + \frac{\gamma S^2}{r_d(\theta_s - \theta_i)} + \frac{(2-\beta)(K_{fs} - K_i)}{3} \right] t \quad [19]$$

where γ and β are constants, with the common assumptions that $\gamma = 0.75$ and $\beta = 0.6$, and K_i is the hydraulic conductivity corresponding to initial pressure head h_i. Brooks and Corey parameters were used to determine sorptivity S (by Eq. [2]) and K_i (by Eq. [10]). The above form of the Haverkamp solution is only valid early on, that is, when time $t < t_{grav}$, where $t_{grav} = S^2/K_{fs}^2$ (Philip, 1969); therefore, values of CV(RMSD) were calculated based on cumulative infiltration (y_{total}) that had occurred at the lesser of time t = 500 min or t_{grav}. Note that t_{grav} differs from the τ_{crit} term defined in Eq. [1], as discussed at the end of the next section.

RESULTS AND DISCUSSION

Synthetic Soils

Scaled capillary length parameter (λ/λ_{max}) was analyzed for eight synthetic soils, four having Brooks and Corey hydraulic parameters and four having van Genuchten parameters. The capillary length λ remains relatively constant and equal to the maximum capillary length (λ_{max}) for much of the dry soil range (Fig. 2a and 2b). When plotted as degree of saturation [Θ_i, where $\Theta_i = (\theta_i - \theta_r)/(\theta_s - \theta_r)$], the ratio λ/λ_{max} is greater than 0.9 for the range $0 \le \Theta_i \le 0.7$ (Fig. 2c and 2d). Previous studies have suggested that λ is constant when soils are initially drier than field capacity (e.g., Scotter et al., 1982); the analysis shown here supports this assumption for most initial conditions and soil types, with the more specific constraints that $\lambda \approx \lambda_{max}$ for $h_i > 2h_b$ (Brooks and Corey parameters) or $h_i > 2/\alpha$ (van Genuchten-Mualem parameters).

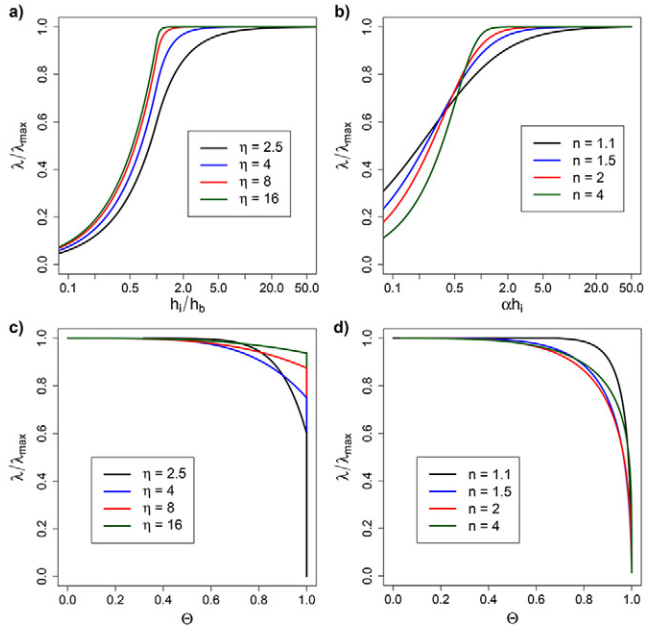

Fig. 2. Relative capillary length (λ/λ_{max}) for four synthetic soils as a function of (a, b) scaled initial matric head and (c, d) initial degree of saturation. Panels (a) and (c) show soils that are characterized using Brooks and Corey hydraulic parameters h_b and η. Panels (b) and (d) show soils characterized with the van Genuchten–Mualem hydraulic parameters α and n.

The magnitude of λ_{max} changes as a function of the Brooks and Corey hydraulic properties h_b and η (Fig. 3a). Based on Eq. [12] and the limitation that $\eta > 2$, λ_{max} varies between $h_b/2$ (as η approaches 2) and h_b (as η becomes large; Fig. 3b). Thus, the magnitude of λ_{max} is primarily controlled by the soil bubbling pressure head h_b.

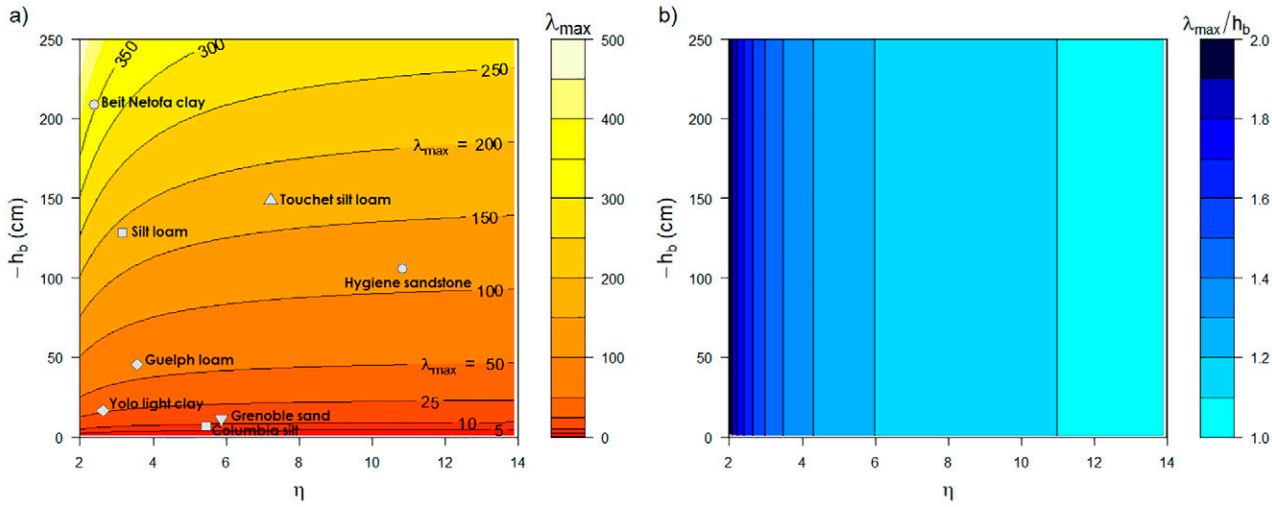

Fig. 3. Predictions of λ_{max} (a) in cm and (b) relative to the Brooks and Corey bubbling pressure head h_b, as functions of pore-size parameter η and h_b. Soils numbered 1 to 8 in Table 1 are plotted in (a) for reference.

HYDRUS-3D Simulations

Equation [8] provided estimates of cumulative infiltration that were similar in magnitude to the HYDRUS results, with all values of CV(RMSD) less than 0.08 for Brooks and Corey parameters (Fig. 4 and 5) and less than 0.25 for van Genuchten parameters (Fig. 4). The Brooks and Corey parameter model therefore provided predictions that better matched the HYDRUS results, with RMSD values that represented less than 8% of the total infiltration amounts. Further, the van Genuchten model predicted less infiltration than the Brooks and Corey model by up to a factor of 4.5 (as seen in Fig. 4d) and with a typical difference of ~2*x*. This discrepancy is potentially due to differences in predicted hydraulic conductivity near saturation, where the van Genuchten–Mualem hydraulic conductivity has been previously shown to under-predict $K(h)$ (Schaap and van Genuchten, 2006; Vogel and Cislerova, 1988).

This difference in near-saturated hydraulic conductivity also resulted in the Brooks and Corey model systematically predicting higher values for f and λ (Table 2) compared with the van Genuchten–Mualem model (Table 3). The only exception is the Columbia silt soil, where we altered the soil hydraulic parameters to obtain equivalent λ_{max} values between the Brooks and Corey and van Genuchten models (Fig. 4f and 4 g). In this instance, Eq. [8] gave similar infiltration predictions for the case when $h_i = -5{,}000$ cm (Fig. 4f). Moreover, those predictions were nearly identical to the HYDRUS results with the Brooks and Corey

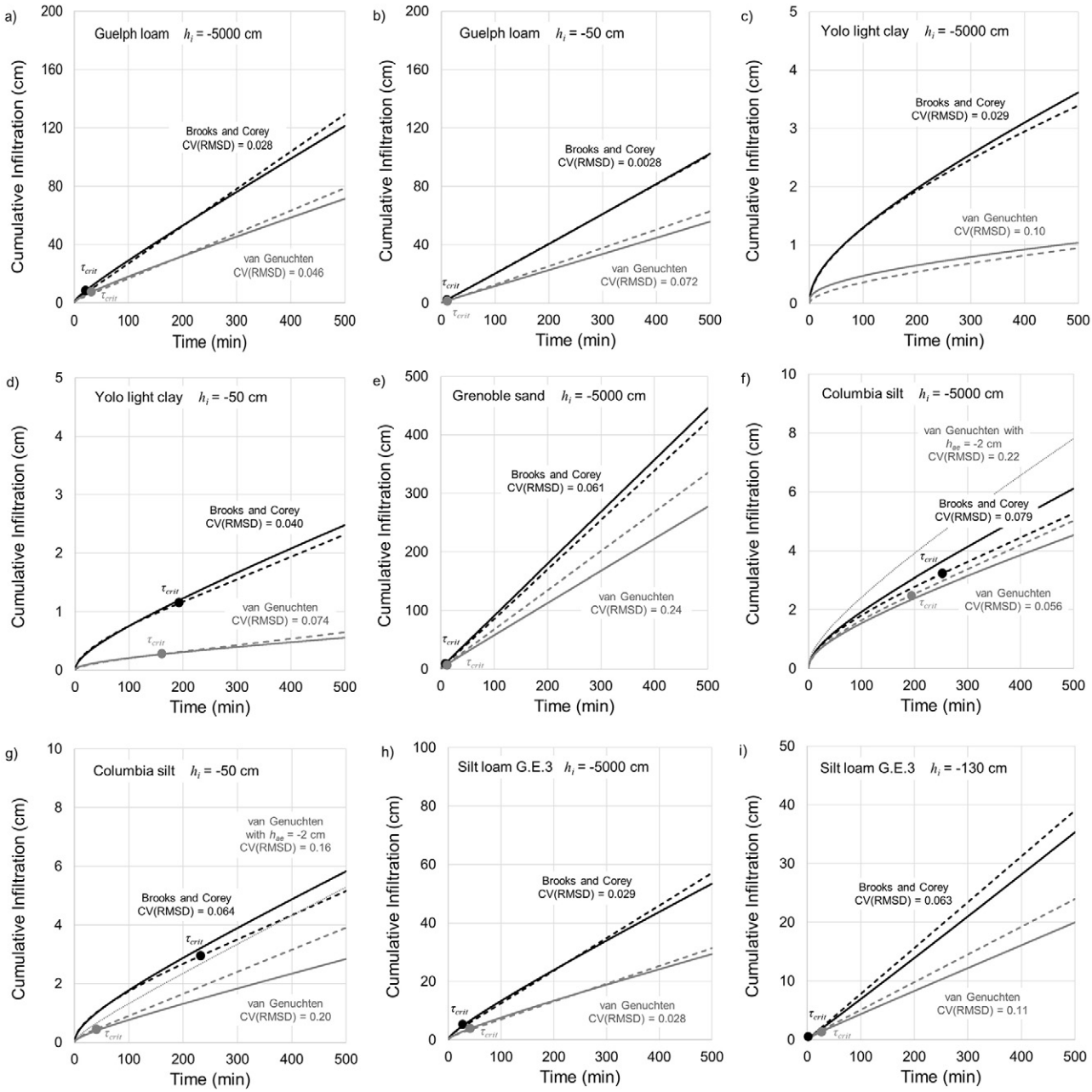

Fig. 4. Predicted infiltration from the tested models for d = 1 cm and h_{source} = 0 cm. Solid lines show HYDRUS-3D simulations (black, Brooks and Corey parameters; gray, van Genuchten–Mualem parameters); dashed lines represent Eq. [8] with Brooks and Corey hydraulic parameters (black) and van Genuchten–Mualem parameters (gray). Dotted gray lines in (f) and (g) represent the van Genuchten–Mualem parameters with the "air-entry = –2 cm" option enabled in HYDRUS.

parameters. However, the HYDRUS predictions using the van Genuchten model again showed less infiltration than the Brooks and Corey or semi-analytical models. When we instead enabled "with air entry value of −2 cm" in HYDRUS, which recreates the modified van Genuchten function recommended by Vogel et al. (2000), the HYDRUS model then predicted the most infiltration in the initially dry conditions (Fig. 4f), and a similar amount of infiltration as the semi-analytical model with van Genuchten parameters for the initially wet conditions (Fig. 4g). This finding provides additional evidence that the van Genuchten model may have considerable uncertainty, particularly for the $K(h)$ function in near-saturated conditions.

The Columbia silt soil tests also revealed that the choice of hydraulic model will affect infiltration predictions in wet conditions, even with an approximately equivalent values for capillary length λ and matric flux potential, Λ. This discrepancy exists because the van Genuchten and Brooks and Corey hydraulic models differ in their estimates of initial water content, which in turn influences the estimates of soil sorptivity. The effect is minor when the soils are initially dry, as the initial water content is generally much smaller than the saturated water content; however, for the wet initial conditions, the two models can diverge in their predictions by a substantial margin. For example, in the aforementioned Columbia Silt experiment, where we matched the matric flux potential term between models, the Brooks and Corey model predicted an initial water content of 0.04 for $h_i = -50$ cm, while the van Genuchten model predicted an initial water content of 0.34 (nearly an order of magnitude

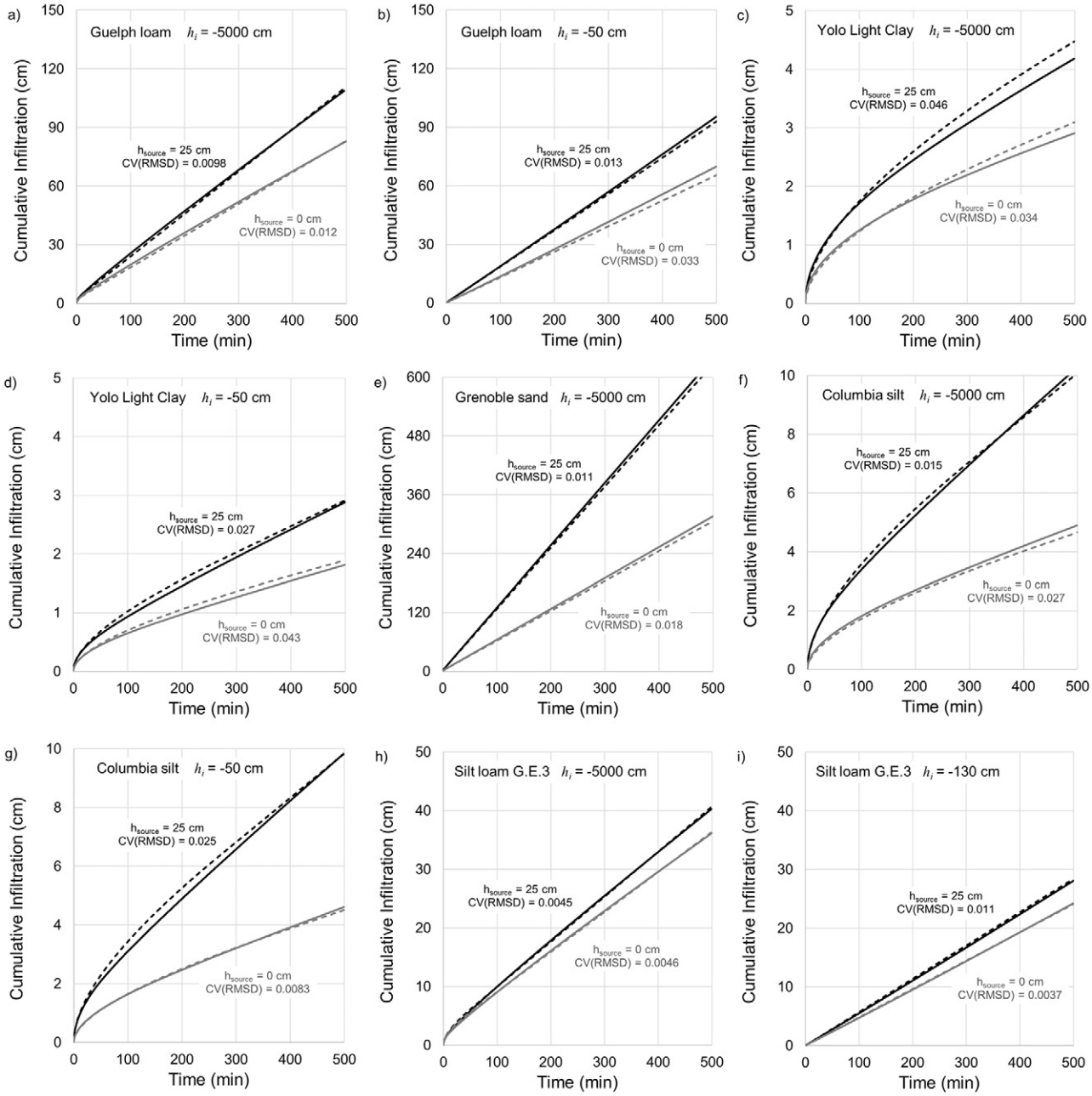

Fig. 5. Predicted infiltration from the tested models for d = 5 cm and h_{source} = 0 cm (gray lines) and h_{source} = 25 cm (black lines). Solid lines show HYDRUS-3D simulations, while dashed lines represent Eq. [8], all using Brooks and Corey hydraulic parameters.

Table 2. Calculated values for capillary length λ (cm; Eq. [3]) and three-dimensional shape factor *f* (Eq. [6]) at various initial pressure heads (h_i) using the Brooks and Corey hydraulic model (Eq. [11] and [14]). The relative capillary length (λ/λ_{max}) is also presented for the high initial water content simulation.

	λ			*f*			λ/λ_{max}
Soil	**Max.**	**h_i = −5000 cm**	**h_i = −50 cm**	**Max.**	**h_i = −5000 cm**	**h_i = −50 cm**	**h_i = −50 cm**
Guelph loam	63.6	63.6	49.5	11.6	11.6	9.23	0.78
Yolo light clay	26.8	26.8	25.1	5.46	5.46	5.18	0.94
Grenoble sand	13.8	13.8	13.8	3.30	3.30	3.30	1.0
Columbia silt	8.15	8.15	8.15	2.36	2.36	2.36	1.0
Silt loam G.E.3†	188	188	130	32.3	32.3	22.7	0.69

† h_i = −130 cm for the high initial water content simulation.

Table 3. Calculated values for capillary length λ (cm; Eq. [3]) and three-dimensional shape factor *f* (Eq. [6]) at various initial pressure head (h_i) using the van Genuchten–Mualem hydraulic model. The relative capillary length (λ/λ_{max}) is also presented for the high water content simulation.

	λ			*f*			λ/λ_{max}
Soil	**Max.**	**h_i = −5000 cm**	**h_i = −50 cm**	**Max.**	**h_i = −5000 cm**	**h_i = −50 cm**	**h_i = −50 cm**
Guelph loam	36.2	36.2	28.2	7.04	7.04	5.70	0.78
Yolo light clay	3.12	3.12	2.91	1.52	1.52	1.49	0.92
Grenoble sand	9.65	9.65	9.56	2.61	2.61	2.59	0.99
Columbia silt	8.15	8.15	6.88	2.36	2.36	2.15	0.84
Silt loam G.E.3†	99.8	99.8	76.2	17.6	17.6	13.7	0.76

† h_i = −130 cm for the high initial water content simulation.

greater). Thus, even in cases where the capillary lengths are set to be equivalent, the models may predict different infiltration rates due to other discrepancies between the hydraulic parameter sets.

Next, we compared Eq. [8] with the Haverkamp et al. (1994) early-time model. The two solutions gave similar predictions for the simulations with shallowly inserted rings (i.e., d = 1 cm). In this case both models matched well with the HYDRUS results, with low to very low CV(RMSD) values (Table 4). However, the Haverkamp et al. (1994) model gave poor predictions for the deeply inserted rings (i.e., d = 5 cm), with CV(RMSD) values compared with the HYDRUS solution of between 0.13 and 0.80 (indicating that the RMSD represented 13 to 80% of predicted infiltration). The Haverkamp et al. (1994) model was originally developed for tension disk sources placed on the soil surface, and does not have the ability to account for increasing ring insertion depths. On the other hand, the relatively low CV(RMSD) values for the d = 1 cm tests suggest that the Haverkamp et al. (1994) solution can be applied to shallowly installed ring infiltrometers, such as when using the BEST analysis (Braud et al., 2005, Lassabatère et al., 2006).

Next, to test the validity of our assumption that a = 0.45, we analyzed the sensitivity of the model results to that parameter (Fig. 6). While some differences existed between the exact a value that minimized the CV(RMSD) for each simulation, in all instances except the Grenoble sand the optimal values occurred over the range $1/3 \le a \le 2/3$. These values are much lower than a = 0.91 recommended by Wu and Pan (1997), and also better align with the range of potential a values suggested by Philip (1990) for one-dimensional infiltration (i.e., $0 \le a \le 2/3$, corresponding to the non-shaded region in Fig. 6). The optimum a value, as determined taking the mean of the optimal a values for the five soils and two insertion depths, was 0.45 if the Grenoble sand was constrained to $a \le 2/3$, or 0.5 if the Grenoble sand was left unconstrained. Thus, while variation in optimal a values exists between different soil types (and likely between different soil water diffusivity functional shapes), a = 0.45 works as a suitable first approximation.

Last, the transition time of the model (τ_{crit}; Eq. [8c]) was defined to ensure continuity in cumulative infiltration and infiltration rate between the early-time and steady-state regimes.

In certain soils and conditions, τ_{crit} predicts transition times on the order of seconds or minutes, though the exact value of τ_{crit} can vary widely depending on the chosen value of the parameter a. For example, with the Silt loam G.E.3 soil simulations (assuming a = 0.45), τ_{crit} was found to be 23 min when h_i = −5,000 cm and less than 1 min when h_i = −130 cm. In contrast, other infiltration models (Haverkamp et al., 1994, Lassabatère et al., 2006) typically rely on a term (deemed t_{grav}) that approximates the time at which transient infiltration solutions begin to diverge. Using the common definition of $t_{grav} = S^2/K_{fs}^2$, t_{grav} is always larger than τ_{crit} (often by two or more orders of magnitude) because in the latter $f \ge 1$ and $a \le 1$. For example, t_{grav} for the Silt loam

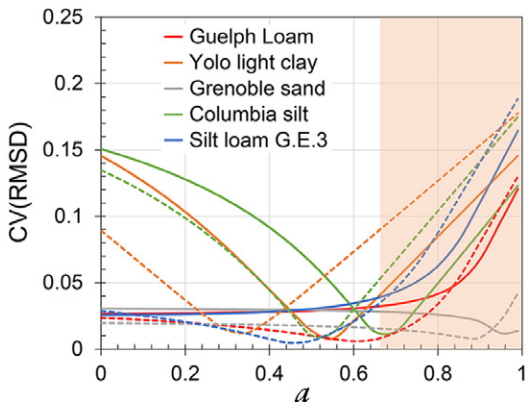

Fig. 6. Sensitivity of the model to parameter a in terms of CV(RMSD) values for five soils analyzed using HYDRUS-3D, with h_{source} = 0 cm and h_i = −5,000 cm. Solid lines indicate ring insertion depth of d = 1 cm; dashed lines indicate d = 5 cm. The shaded region indicates a values >2/3, which are not physically possible (for one-dimensional vertical infiltration) based on the analysis of Philip (1990).

Table 4. Comparison of coefficient of variation of the root mean square deviation, CV(RSMD), between cumulative infiltration predicted by HYDRUS and by Eq. [8] versus the "early-time" version of the Haverkamp et al. (1994) model. Brooks and Corey parameters shown in Table 2 were used.

Soil	h_i	d	h_{source}	τ_{crit}	t_{grav}	CV(RSMD)	
						Eq. [8]	Haverkamp et al.
	cm			min			
Guelph loam	−5000	1	0	10.3	1.68×10^3	0.028	0.0015
Guelph loam	−5000	5	0	25.5	1.68×10^3	0.012	0.27
Guelph loam	−5000	5	25	19.8	2.37×10^3	0.0098	0.28
Guelph loam	−50	1	0	0.614	63.3	0.0028	0.033
Guelph loam	−50	5	0	1.48	63.3	0.033	0.23
Guelph loam	−50	5	25	1.11	95.4	0.013	0.97
Yolo light clay	−5000	1	0	627	2.26×10^4	0.029	0.070
Yolo light clay	−5000	5	0	1380	2.26×10^4	0.035	0.21
Yolo light clay	−5000	5	25	949	4.38×10^4	0.046	0.29
Yolo light clay	−50	1	0	193	6.26×10^3	0.040	0.078
Yolo light clay	−50	5	0	421	6.26×10^3	0.043	0.31
Yolo light clay	−50	5	25	286	1.25×10^4	0.027	0.36
Grenoble sand	−5000	1	0	2.32	30.5	0.030	0.041
Grenoble sand	−5000	5	0	4.46	30.5	0.018	0.14
Grenoble sand	−5000	5	25	2.98	85.8	0.011	0.20
Grenoble sand	−50	1	0	1.97	26.0	0.029	0.039
Grenoble sand	−50	5	0	3.79	26.0	0.019	0.13
Grenoble sand	−50	5	25	2.54	73.0	0.012	0.059
Columbia silt	−5000	1	0	252	1.69×10^3	0.079	0.0092
Columbia silt	−5000	5	0	425	1.69×10^3	0.027	0.13
Columbia silt	−5000	5	25	306	6.88×10^3	0.015	0.30
Columbia silt	−50	1	0	227	1.53×10^3	0.064	0.020
Columbia silt	−50	5	0	383	1.53×10^3	0.0083	0.16
Columbia silt	−50	5	25	276	6.21×10^3	0.025	0.33
Silt loam G.E.3	−5000	1	0	22.7	2.87×10^4	0.029	0.054
Silt loam G.E.3	−5000	5	0	60.6	2.87×10^4	0.0046	0.36
Silt loam G.E.3	−5000	5	25	54.1	3.26×10^4	0.0045	0.37
Silt loam G.E.3	−130	1	0	0.191	119	0.064	0.0085
Silt loam G.E.3	−130	5	0	0.502	119	0.0037	0.25
Silt loam G.E.3	−130	5	25	0.431	142	0.011	0.80

G.E.3 soil was calculated to be 2.8×10^4 minutes for the dry initial conditions and 119 min for the wet conditions. Similarly, the Yolo light clay soil with initially wet conditions had a τ_{crit} value of 190 min versus a t_{grav} value of 6.3×10^3 minutes. Altogether, nine of the ten simulations had τ_{crit} values less than 500 min (the length of the simulation period), meaning that the steady-state solution was applicable in nearly every instance. The low CV(RMSD) values given between Eq. [8] and the HYDRUS simulations indicate that τ_{crit} is an appropriate parameter to estimate time to steady -state flow, and that fine-textured soils may reach steady-state conditions in relatively short time-scales (minutes to hours).

The water supply ponding depth also influenced the values of τ_{crit} and t_{grav} in opposite ways. Specifically, higher h_{source} values caused τ_{crit} to decrease and t_{grav} to increase (Table 4). This result is because τ_{crit}, as defined in Eq. [8c], has h_{source} in the numerator and $(h_{source})^2$ in the denominator (being implicit within the f^2 term), whereas in t_{grav} the h_{source} term only affects the numerator (being implicit to the S^2 term). As a consequence, τ_{crit} may be particularly useful in determining time to a steady state when high water supply pressures are used.

SUMMARY AND CONCLUSIONS

In this study, we modified and combined two infiltration models (Reynolds and Elrick, 1990, Wu et al., 1999) to generate a new comprehensive model for single ring infiltration (Eq. [8]). Cumulative infiltration predictions were compared with results from HYDRUS-3D using both the Brooks and Corey and the van Genuchten-Mualem hydraulic parameter sets. With either parameterization, the infiltration model gave accurate results for different initial conditions (i.e., wet and dry soil) and experimental settings (i.e., varying ring insertion and water ponding depths). We also examined predictions of the capillary length (λ) and wetting shape parameter (f) using both hydraulic parameter models. The van Genuchten–Mualem parameters provided relatively low predictions of λ and f (and, as a result, low predictions for cumulative infiltration), due to underestimation of near-saturated hydraulic conductivity. The van Genuchten-Mualem model also required numerical integration to use, whereas the Brooks and Corey parameterization resulted in explicit expressions for λ and f, thus facilitating ease of use. Still, certain soils may not be well described using traditional hydraulic models (e.g., Brooks and Corey or van Genuchten-Mualem), which will limit the accuracy of analytical solutions for estimating λ (and f). In such instances it may be preferable to parameterize λ using in situ measurements, such as those given by the Bouwer in-

filtrometer (Bouwer, 1966), or based on suggested values per soil texture and structure (Reynolds et al., 2002).

The proposed analytical expressions were also valuable for exploring the role of soil hydraulic properties and initial water content/matric potential in determining cumulative infiltration from a single ring source. We showed that the capillary length (λ) is approximately constant for dry initial conditions. Specifically, when the scaled initial matric head (e.g., h_i/h_b using Brooks and Corey parameters, or αh_i using van Genuchten parameters) is greater than approximately two, the capillary length is within 10% of its maximum value (λ_{max}) regardless of soil properties. In terms of degree of saturation (Θ_i), the capillary length is within 10% of λ_{max} for all soils so long as Θ_i is less than 0.7. This finding means that when analyzing most infiltration tests (which are typically conducted during moderately wet to dry conditions), the capillary length and matric flux potential can be assumed constant. As such, we proposed a simplified expression that requires only estimates of the soil water retention parameters, hydraulic conductivity, and information about the single ring source (i.e., radius, depth of insertion, ponded depth) to use. Altogether, the infiltration model developed in this study is simple, easy to parameterize and interpret, applicable to most initial conditions and soil types with minimal error, and capable of describing both early-time and steady-state infiltration behaviors.

ACKNOWLEDGMENTS

Funding for this work was provided by the USDA–NRCS Conservation Innovation Grant No. 69-3A75-14-260. Funding was also provided in part by the USDA–NRCS Virginia Agricultural Experiment Station and the Hatch Program of the USDA National Institute of Food and Agriculture.

REFERENCES

Angulo-Jaramillo, R., V. Bagarello, M. Iovino, and L. Lassabatere. 2016. Infiltration measurements for soil hydraulic characterization. Springer, Switzerland. doi:10.1007/978-3-319-31788-5.

Bouwer, H. 1966. Rapid field measurement of air entry value and hydraulic conductivity of soil as significant parameters in flow system analysis. Water Resour. Res. 2:729–738. doi:10.1029/WR002i004p00729

Braud, I., D. De Condappa, J.M. Soria, R. Haverkamp, R. Angulo-Jaramillo, S. Galle, et al. 2005. Use of scaled forms of the infiltration equation for the estimation of unsaturated soil hydraulic properties (the Beerkan method). Eur. J. Soil Sci. 56:361–374. doi:10.1111/j.1365-2389.2004.00660.x

Brooks, R.H., and A.T. Corey. 1964. Hydraulic properties of porous media. Hydrology Papers. Colorado State University, Ft. Collins, CO.

Castellini, M., M. Iovino, M. Pirastru, M. Niedda, and V. Bagarello. 2016. Use of BEST procedure to assess soil physical quality in the Baratz Lake Catchment (Sardinia, Italy). Soil Sci. Soc. Am. J. 80:742–755. doi:10.2136/sssaj2015.11.0389

Di Prima, S., V. Bagarello, L. Lassabatere, R. Angulo-Jaramillo, I. Bautista, M. Burguet, et al. 2017. Comparing Beerkan infiltration tests with rainfall simulation experiments for hydraulic characterization of a sandy-loam soil. Hydrol. Processes. doi:10.1002/hyp.11273

Elrick, D., and W. Reynolds. 1992. Methods for analyzing constant-head well permeameter data. Soil Sci. Soc. Am. J. 56:320–323. doi:10.2136/sssaj1992.03615995005600010052x

Fatehnia, M., K. Tawfiq, and M. Ye. 2016. Estimation of saturated hydraulic conductivity from double-ring infiltrometer measurements. Eur. J. Soil Sci. 67:135–147. doi:10.1111/ejss.12322

Fuentes, C., R. Haverkamp, and J.Y. Parlange. 1992. Parameter constraints on closed-form soilwater relationships. J. Hydrol. 134:117–142. doi:10.1016/0022-1694(92)90032-Q

Gardner, W. 1958. Some steady-state solutions of the unsaturated moisture flow equation with application to evaporation from a water table. Soil Sci. 85:228–232. doi:10.1097/00010694-195804000-00006

Haverkamp, R., J.-Y. Parlange, J. Starr, G. Schmitz, and C. Fuentes. 1990. Infiltration under ponded conditions: 3. A predictive equation based on physical parameters. Soil Sci. 149:292–300. doi:10.1097/00010694-199005000-00006

Haverkamp, R., P.J. Ross, K.R.J. Smettem, and J.Y. Parlange. 1994. Three-dimensional analysis of infiltration from the disc infiltrometer: 2. Physically based infiltration equation. Water Resour. Res. 30:2931–2935. doi:10.1029/94WR01788

Hinnell, A.C., N. Lazarovitch, and A.W. Warrick. 2009. Explicit infiltration function for boreholes under constant head conditions. Water Resour. Res. 45. doi:10.1029/2008WR007685

Lassabatère, L., R. Angulo-Jaramillo, J.M. Soria Ugalde, R. Cuenca, I. Braud, and R. Haverkamp. 2006. Beerkan estimation of soil transfer parameters through infiltration experiments–BEST. Soil Sci. Soc. Am. J. 70:521–532. doi:10.2136/sssaj2005.0026

Philip, J.R. 1957. The theory of infiltration: 1. The infiltration equation and its solution. Soil Sci. 83:345. doi:10.1097/00010694-195705000-00002

Philip, J.R. 1969. Theory of infiltration. Advances in Hydroscience 5:215–296. doi:10.1016/B978-1-4831-9936-8.50010-6

Philip, J.R. 1984. Steady infiltration from circular cylindrical cavities. Soil Sci. Soc. Am. J. 48:270–278. doi:10.2136/sssaj1984.03615995004800020008x

Philip, J.R. 1987. The infiltration joining problem. Water Resour. Res. 23:2239–2245. doi:10.1029/WR023i012p02239

Philip, J.R. 1990. Inverse solution for one-dimensional infiltration, and the ratio a/K1. Water Resour. Res. 26:2023–2027.

Pollalis, E.D., and J.D. Valiantzas. 2014. Isolation of a 1D infiltration time interval under ring infiltrometers for determining sorptivity and saturated hydraulic conductivity: Numerical, theoretical, and experimental approach. J. Irrig. Drain. Eng. 141:04014050. doi:10.1061/(asce)ir.1943-4774.0000796

Reynolds, W., and D. Elrick. 1990. Ponded infiltration from a single ring: I. Analysis of steady flow. Soil Sci. Soc. Am. J. 54:1233–1241. doi:10.2136/sssaj1990.03615995005400050006x

Reynolds, W., and D. Elrick. 1991. Determination of hydraulic conductivity using a tension infiltrometer. Soil Sci. Soc. Am. J. 55:633–639. doi:10.2136/sssaj1991.03615995005500030001x

Reynolds, W., D. Elrick and E. Youngs. 2002. Ring or cylinder infiltrometers (vadose zone). In: J.H. Dane, and G.C. Topp, editors, Methods of soil analysis. Part 4. SSSA Book Ser. 5. SSSA, Madison, WI. p. 818–826.

Schaap, M.G., and M.T. van Genuchten. 2006. A modified Mualem–van Genuchten formulation for improved description of the hydraulic conductivity near saturation. Vadose Zone J. 5:27–34. doi:10.2136/vzj2005.0005

Scotter, D., B. Clothier, and E. Harper. 1982. Measuring saturated hydraulic conductivity and sorptivity using twin rings. Soil Res. 20:295–304. doi:10.1071/SR9820295

Shuster, W.D., S.D. Dadio, C.E. Burkman, S.R. Earl, and S.J. Hall. 2015. Hydropedological assessments of parcel level infiltration in an arid urban ecosystem. Soil Sci. Soc. Am. J. 79:398. doi:10.2136/sssaj2014.05.0200

Stewart, R.D., D.E. Rupp, M.R.A. Najm, and J.S. Selker. 2013. Modeling effect of initial soil moisture on sorptivity and infiltration. Water Resour. Res. 49:7037–7047. doi:10.1002/wrcr.20508

van Genuchten, M.T. 1980. A closed-form equation for predicting the hydraulic conductivity of unsaturated soils. Soil Sci. Soc. Am. J. 44:892–898. doi:10.2136/sssaj1980.03615995004400050002x

Vogel, T., and M. Cislerova. 1988. On the reliability of unsaturated hydraulic conductivity calculated from the moisture retention curve. Transp. Porous Media 3:1–15. doi:10.1007/BF00222683

Vogel, T., M.T. Van Genuchten, and M. Cislerova. 2000. Effect of the shape of the soil hydraulic functions near saturation on variably-saturated flow predictions. Adv. Water Resour. 24:133–144. doi:10.1016/S0309-1708(00)00037-3

White, I., and M. Sully. 1987. Macroscopic and microscopic capillary length and time scales from field infiltration. Water Resour. Res. 23:1514–1522. doi:10.1029/WR023i008p01514

Wooding, R. 1968. Steady infiltration from a shallow circular pond. Water Resour. Res. 4:1259–1273. doi:10.1029/WR004i006p01259

Wu, L., and L. Pan. 1997. A generalized solution to infiltration from single-ring infiltrometers by scaling. Soil Sci. Soc. Am. J. 61:1318–1322. doi:10.2136/sssaj1997.03615995006100050005x

Wu, L., L. Pan, J. Mitchell, and B. Sanden. 1999. Measuring saturated hydraulic conductivity using a generalized solution for single-ring infiltrometers. Soil Sci. Soc. Am. J. 63:788–792. doi:10.2136/sssaj1999.634788x